

Alma Mater Studiorum Università di Bologna
Archivio istituzionale della ricerca

Determination of a semi-experimental equilibrium structure of 1-phosphapropyne from millimeter-wave spectroscopy of CH₃CP and CD₃CP

This is the final peer-reviewed author's accepted manuscript (postprint) of the following publication:

Published Version:

Degli Esposti, C., Melosso, M., Bizzocchi, L., Tamassia, F., Dore, L. (2020). Determination of a semi-experimental equilibrium structure of 1-phosphapropyne from millimeter-wave spectroscopy of CH₃CP and CD₃CP. JOURNAL OF MOLECULAR STRUCTURE, 1203, 1-9 [10.1016/j.molstruc.2019.127429].

Availability:

This version is available at: <https://hdl.handle.net/11585/722038> since: 2020-02-05

Published:

DOI: <http://doi.org/10.1016/j.molstruc.2019.127429>

Terms of use:

Some rights reserved. The terms and conditions for the reuse of this version of the manuscript are specified in the publishing policy. For all terms of use and more information see the publisher's website.

This item was downloaded from IRIS Università di Bologna (<https://cris.unibo.it/>).
When citing, please refer to the published version.

(Article begins on next page)

This is the final peer-reviewed accepted manuscript of:

Determination of a semi-experimental equilibrium structure of 1-phosphapropyne from millimeter-wave spectroscopy of CH₃CP and CD₃CP | Elsevier Enhanced Reader [WWW Document], n.d.

The final published version is available online at:
<https://doi.org/10.1016/j.molstruc.2019.127429>

Terms of use:

Some rights reserved. The terms and conditions for the reuse of this version of the manuscript are specified in the publishing policy. For all terms of use and more information see the publisher's website.

This item was downloaded from IRIS Università di Bologna (<https://cris.unibo.it/>)

When citing, please refer to the published version.

Determination of a Semi-Experimental Equilibrium Structure of 1-phosphapropyne from Millimeter-wave Spectroscopy of CH₃CP and CD₃CP

Claudio Degli Esposti^a, Mattia Melosso^{a,*}, Luca Bizzocchi^b, Filippo Tamassia^c, Luca Dore^a

^a*Dipartimento di Chimica "Giacomo Ciamician", Università di Bologna, Via F. Selmi 2, I-40126 Bologna (Italy)*

^b*Center for Astrochemical Studies, Max Planck Institut für extraterrestrische Physik Gießenbachstraße 1, D-85748 Garching bei München (Germany)*

^c*Dipartimento di Chimica Industriale "Toso Montanari", Università di Bologna, Viale del Risorgimento 4, I-40136 Bologna, Italy*

Abstract

Trideuterated 1-phosphapropyne (CD₃CP) has been produced by co-pyrolysis of phosphorus trichloride and esadeuterated ethane. The rotational spectra of CD₃CP in the ground and the low-lying vibrational states ν_8 (CCP bending mode) and $2\nu_8$ have been investigated in the millimeter-wave region. Very accurate values of the quartic centrifugal distortion constants D_J and D_{JK} and of the sextic distortion constants H_{JK} and H_{KJ} have been obtained for the ground state. l -type resonance effects have been taken into account in the analysis of the spectra of the degenerate bending states, so that the energy difference between the $\nu_8^{|l|} = 2^0$, and $\nu_8^{|l|} = 2^2$ states could be determined, together with a number of spectroscopic constants involved in the l -type resonance. Moreover, for the parent isotopologue CH₃CP a new set of excited-state lines ($\nu_8 = 1, 2$ and $\nu_4 = 1$) were recorded up to 330 GHz, and a global analysis including all available rotational and rovibrational transitions related to the ground and $\nu_8 = 1, 2$ states has been performed. A satisfactory fit could only be obtained by making a reassignment of the few transition wavenumbers previously measured for the $2\nu_8^0 \leftarrow \nu_8^{\pm 1}$ hot band [M.K. Bane, *et al.*, *J. Mol. Spectrosc.* **275** (2012) 9–14].

The experimental work has been combined with quantum-chemical computations. Quadratic and cubic force constants of 1-phosphapropyne have been calculated at MP2 level of theory with a basis set of triple- ζ quality. A semi-experimental equilibrium structure has been derived by correcting experimental ground-state rotational constants by means of theoretical vibration-rotation interaction constants.

Keywords: Equilibrium structure, Pyrolysis, Rotational Spectroscopy, Millimeter-Wave, Coupled Cluster Calculation

1. Introduction

1-phosphapropyne (CH₃CP, IUPAC name ethyldynephosphine) is a semi-stable molecule which was first detected by microwave [1] and photoelectron spectroscopy [2] in the pyrolysis products of ethyldichlorophosphine (CH₃CH₂PCl₂). The rotational spectrum of several isotopologues of 1-phosphapropyne was studied by Kroto *et al.* [3] in the 26–40 GHz frequency range, where the $J = 3 \leftarrow 2$ and $J = 4 \leftarrow 3$ rotational transitions for the most abundant isotopologue, and the $J = 4 \leftarrow 3$ transition for CD₃CP were detected. Medium-resolution, infra-red (IR) studies of the vibrational spectra of CH₃CP and CD₃CP were performed by Ohno *et al.* [4, 5, 6, 7, 8, 9]. Later, the ground state rotational spectra of normal CH₃CP and the

^{*}Supplementary material available.

^{*}Corresponding author

Email address: mattia.melosso2@unibo.it (Mattia Melosso)

isotopic variants $^{13}\text{CH}_3\text{CP}$ and CH^{13}CP have been observed by Bizzocchi *et al.* [10] in the millimeter and submillimeter-wave regions (measurements up to 460 and 195 GHz were performed for the normal and ^{13}C containing species, respectively) obtaining very accurate values of the quartic centrifugal distortion constants D_J and D_{JK} and of the sextic distortion constants H_{JK} and H_{KJ} . A novel preparation route, based on the gas-phase pyrolysis of ethane (CH_3CH_3) and phosphorus trichloride (PCl_3) mixtures was employed in Ref. [10] to produce CH_3CP . More recently, high-resolution spectra of 1-phosphapropyne have been recorded on the far-infrared beamline at the Australian synchrotron between 50 and 400 cm^{-1} [11]. Ro-vibrational transitions of the ν_8 fundamental (308 cm^{-1}) as well as of the $2\nu_8 \leftarrow \nu_8$ hot-band have been assigned, and rotational, centrifugal distortion and Coriolis interaction parameters determined.

The present paper extends to the mm-wave region the study of the rotational spectrum of the isotopic variant CD_3CP in the ground and in the degenerate vibrational excited states ν_8 and $2\nu_8$, and also enlarges considerably the set of data for the low-lying excited states of the normal isotopologue CH_3CP , for which a global analysis including all available rotational and rovibrational transitions related to the ν_8 and $2\nu_8$ states is presented. In addition, the anharmonic force field of 1-phosphapropyne has been calculated at the MP2 level of theory with a triple- ζ basis set. Combining the experimental ground-state rotational constants with calculated vibrational corrections, a semi-experimental equilibrium structure of 1-phosphapropyne has been derived, which agrees well with the *ab initio* structure calculated at the CCSD(T) level of theory using a basis set of quadruple- ζ quality and the core-valence correlation energy gradient correction using the cc-pCVTZ basis set.

2. Experimental Section

Trideuterated 1-phosphapropyne was produced by the gas-phase, high-temperature reaction between phosphorus trichloride and d_6 -ethane already employed by Bizzocchi *et al.* [10]. The precursors were flowed through a heated quartz tube connected to the free-space cell of the millimeter-wave spectrometer, in the same apparatus used to study other unstable species [12, 13, 14]. The yield of the reaction was sufficient to easily observe the ground-state rotational transitions of CD_3CP during the pyrolysis process. The strongest signals due to CD_3CP were obtained by pyrolyzing at 1100 °C a gaseous mixture with a 2:1 excess of PCl_3 at a total pressure of *ca.* 150 mTorr in the quartz reactor, corresponding to *ca.* 15 mTorr of gaseous products flowing continuously in the 3 m long, 10 cm in diameter, glass-made absorption cell of the spectrometer. Figure 1 shows the recording of the ground state, $J = 10 \leftarrow 9$ transition of CD_3CP , as obtained during its high-temperature production.

Since 1-phosphapropyne is a semi-stable compound, the products of the pyrolysis reaction were entirely collected in a liquid-nitrogen-cooled trap placed between the end of the absorption cell and the pumping system, and then roughly purified as described in [10]. The purified material was permanently stored in liquid nitrogen and subsequently used to record the spectra of CD_3CP in vibrationally excited states. Further measurements were also performed for the excited states of the normal isotopologue CH_3CP , in order to include in the available data-set rotational transitions corresponding to higher J values. The rotational spectra were recorded in selected frequency regions between 77 and 524 GHz, using a millimeter/submillimeter-wave spectrometer [15] whose radiation sources are several Gunn diodes (Radiometer Physics GmbH, J.E. Carlstrom Co) which emit in the range 75–134 GHz. Higher frequencies were obtained by using passive multipliers (tripler, quadrupler and sextupler). The output frequency was stabilized by a Phase-Lock-Loop (PLL) system referred to a signal of 75 MHz and modulated at 6 kHz. Phase-sensitive detection at twice the modulation frequency was employed, so that the $2f$ spectrum profile was recorded. Two Schottky barrier diode detectors (Millitech and VDI) were used to record the spectra.

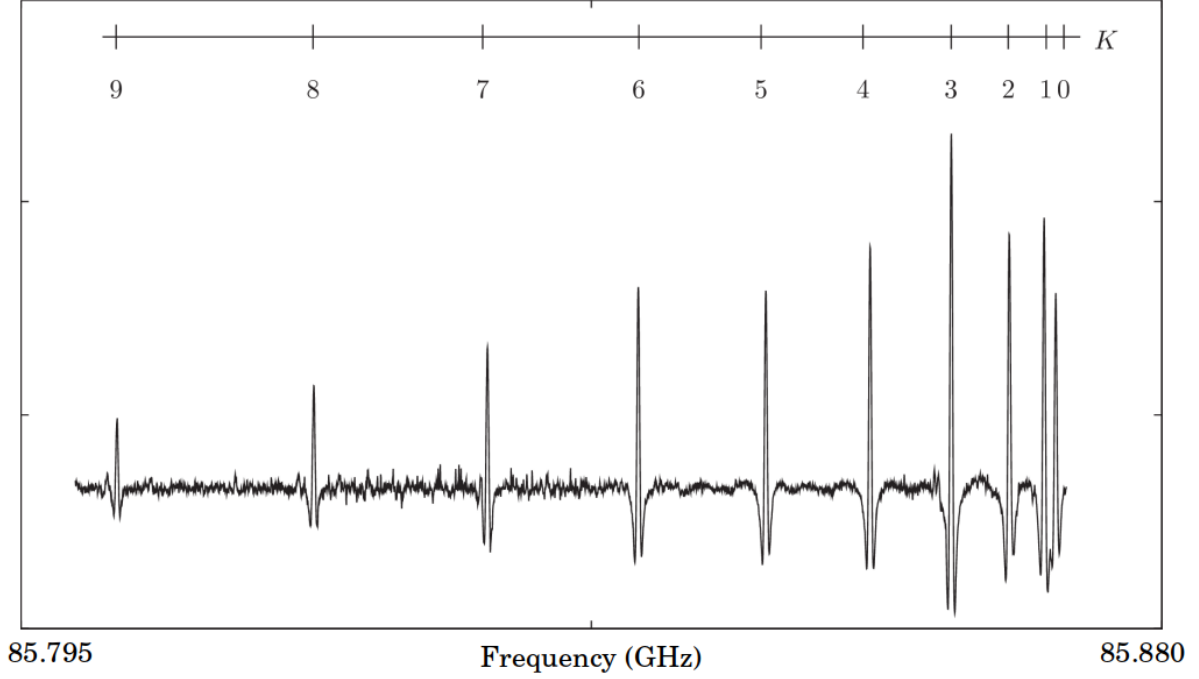


Figure 1: The full K -structure of the $J = 10 \leftarrow 9$ transition of CD_3CP in its ground vibrational state.

3. Theory

The standard ro-vibrational energy for a prolate symmetric-top molecule in non-degenerate vibrational states, including centrifugal distortion terms up to the sextic ones, is [16]:

$$E(v, J, K) = E_v + BJ(J+1) + (A-B)K^2 - D_J[J(J+1)]^2 - D_{JK}[J(J+1)]K^2 - D_KK^4 + H_J[J(J+1)]^3 + H_{JK}[J(J+1)]^2K^2 + H_{KJ}[J(J+1)]K^4 + H_KK^6 \quad (1)$$

The selection rules for rotational transitions are $\Delta J = +1$ and $\Delta K = 0$. It is well known that when a degenerate vibrational mode is considered, an additional quantum number l ($l = v, v-2, v-4, \dots, -v$) must be included. In such a case, the ro-vibrational energies for a given (v, l) state are the eigenvalues of matrices which have diagonal elements of the form [17]:

$$E^{|l|}(v, J, K) = E_v^{|l|} + B^{|l|}J(J+1) + (A^{|l|} - B^{|l|})K^2 - D_J^{|l|}J^2(J+1)^2 - D_{JK}^{|l|}J(J+1)K^2 - D_K^{|l|}K^4 + H_J^{|l|}J^3(J+1)^3 + H_{JK}^{|l|}J^2(J+1)^2K^2 + H_{KJ}^{|l|}J(J+1)K^4 + H_K^{|l|}K^6 - 2(A\zeta)Kl + [\eta_JJ(J+1) + \eta_KK^2 + \tau_JJ^2(J+1)^2 + \tau_{JK}J(J+1)K^2 + \tau_KK^4]Kl \quad (2)$$

where $E_v^{|l|}$ is the pure vibrational energy for the (v, l) state. The $-2(A\zeta)Kl$ term corresponds to the first-order, z -axis Coriolis coupling contribution to the energy of each ro-vibrational level, while the η and τ coefficients describe the corresponding centrifugal distortion corrections. Since the Kl product can take positive and negative values, the leading Coriolis coupling term causes a doublet splitting of each $|K|$ level when both K and l are different from zero. Each component retains a double degeneracy, because the same sign of the product Kl can be obtained using two different combinations of signs for K and l . A further energy contribution is given by rotational l -type resonance, due to x - and y -axis Coriolis coupling, which

generates off-diagonal matrix elements connecting sub-levels with different l values ($\Delta l = \pm 2$, $\Delta K = \pm 2$) within a given degenerate vibrational state [18]:

$$\langle v, J, K, l | H | v, J, K \pm 2, l \pm 2 \rangle = \frac{1}{4} \{ q - q_J J(J+1) + q_K K^2 + q_{KK} K^4 \} \\ \times \{ [J(J+1) - K(K \pm 1)] [J(J+1) - (K \pm 1)(K \pm 2)] [v+l+1 \pm 1] [v-l+1 \mp 1] \}^{\frac{1}{2}} \quad (3)$$

It is to be noted that the matrix elements of Eq. (3) connect only states with the same value of $K-l$. The splittings observed in (Figs. 2-3) arise from l -type resonance and centrifugal distortion effects, which lift the vibrational degeneracy.

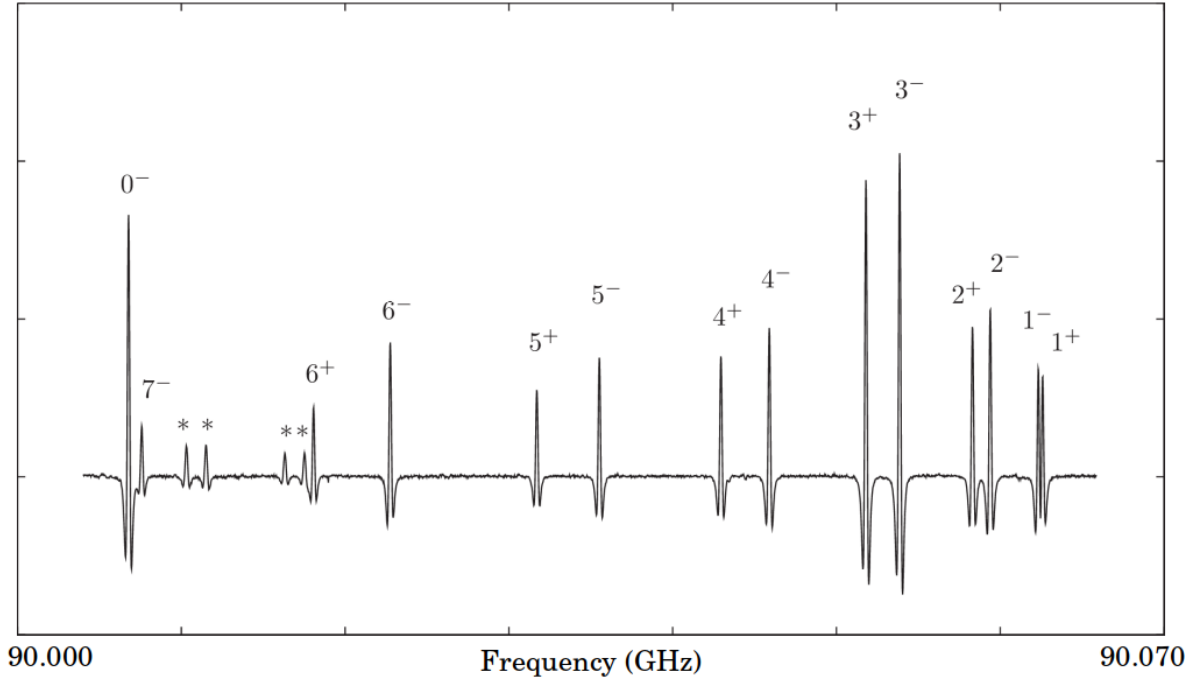


Figure 2: Excerpt of the $J = 9 \leftarrow 8$ transition of CH_3CP in the $v_8 = 1$ state. Each transitions is labeled using the absolute value of $K-l$ and the sign of Kl as superscript. Not all components are shown in the figure. The asterisks mark unassigned lines.

Since the energy displacement produced by the off-diagonal matrix elements of Eq. (3) depends also on the energy separation between the connected levels, the observation of l -type resonance effects for pure rotational transitions with $K-l \neq 0$ in $v = 1$ provides some information also for the $A\zeta$ constant and related centrifugal distortion terms. Finally, it can be noted that in excited bending states both the vibrational energy and the rotational parameters have a dependence on the absolute value of the quantum number l , which can be expressed as $X^{|l|} = X + X_l l^2$. The coefficient X_l is frequently indicated as g_l for the vibrational energy $E_v^{|l|}$ and as γ_l^B for the rotational constant B .

4. Analysis of the spectra

Line frequencies corresponding to the $J = 4 \leftarrow 3$ transition of CD_3CP in the ground and $v_8 = 1, 2$ excited states were first measured in the cm-wave region by Kroto *et al.* [3], so that the identification of new mm-wave lines was straightforward. Further 172 ground-state rotational transitions have been recorded, with J values from 8 to 61, and K values from 0 to 15. The $v_8 = 1, 2$ excited states of CD_3CP were studied

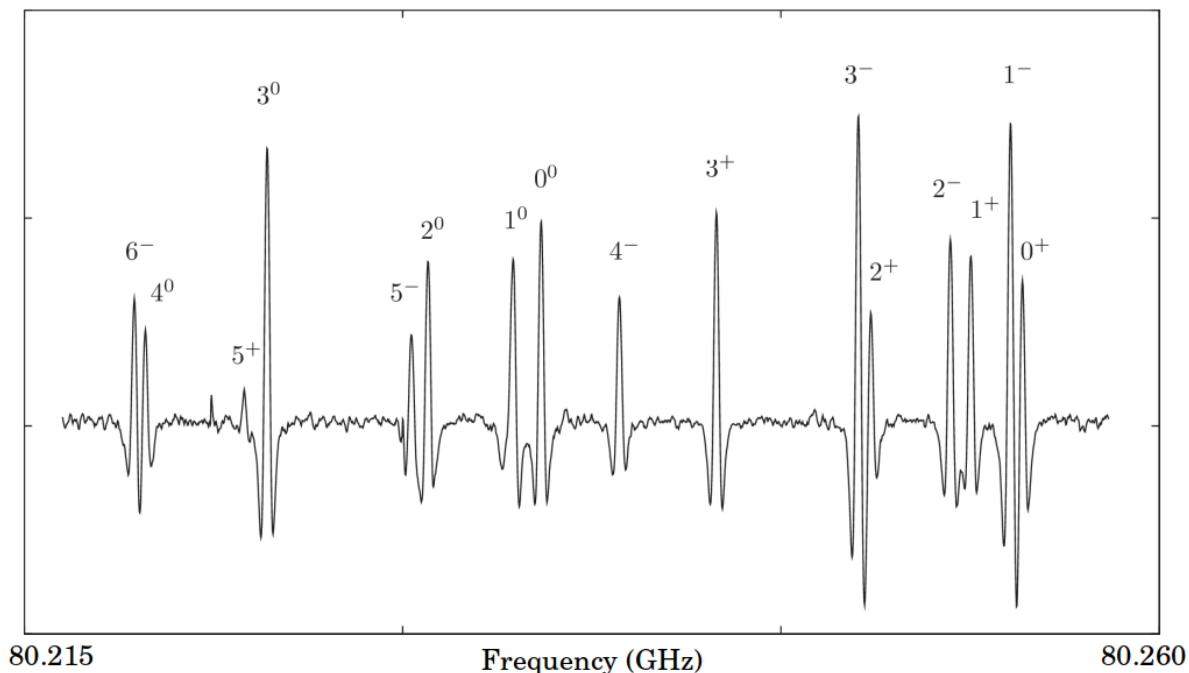


Figure 3: Portion of the $J = 8 \leftarrow 7$ transition of CH_3CP in its $\nu_8 = 2$ state. Each transition is labeled using the absolute value of $K - l$ and the sign of Kl as superscript (when $l=0$, the superscript 0 is used).

in a reduced frequency interval, with J ranging from 8 to 14, and from 9 to 13 for $\nu_8 = 1$ and $\nu_8 = 2$, respectively. The highest K value was 10 for both states. Regarding the CH_3CP main isotopologue, the present investigation extends the previous cm-wave data [3] for the $\nu_8 = 1, 2$ excited states into the 80–111 and 260–330 GHz frequency ranges. In addition, the rotational spectrum of the $\nu_4 = 1$ state (C-C stretching, $\simeq 750 \text{ cm}^{-1}$) was assigned.

The transition frequencies measured for the ground state of CD_3CP and for the $\nu_4 = 1$ state of CH_3CP were analyzed using the energy expression given by Eq. (1). Eqs. (2)–(3) were instead used to analyze the transition frequencies measured for the degenerate states $\nu_8 = 1, 2$ of both CD_3CP and CH_3CP isotopologues. The spectroscopic parameters have been obtained through a nonlinear least-squares fitting procedure, which was performed using Pickett’s SPCAT/SPFIT suite of programs [19]. A large number of ro-vibrational data for the ν_8 fundamental as well as the $2\nu_8 \leftarrow \nu_8$ hot-band were also available for CH_3CP [11], so that a global analysis including microwave and IR transition frequencies could be performed. For CD_3CP , the literature data in the cm-wave region of Ref. [3] have been added to the set of mm- and submm-wave frequencies of the present investigation. Each experimental datum has been weighted proportionally to the inverse square of its experimental uncertainty. Uncertainties of 10–25 kHz were normally assigned to the measurements of the present work, while a larger uncertainty of 40 kHz was chosen for the cm-wave measurements of Ref. [3]. The spectroscopic constants determined for CD_3CP in the ground and $\nu_8 = 1, 2$ excited states are collected in Table 1, where previous results are also shown for comparison.

Very precise values of the rotational constant B and of the quartic centrifugal distortion constants D_J and D_{JK} were obtained for CD_3CP in all the investigated states. In addition, the ground-state values of the sextic distortion constants H_{JK} and H_{KJ} could be determined with great accuracy. H_J does not give a significant contribution to the measured frequencies, and it was therefore constrained to zero in the least-squares analyses. Since the CD_3CP data consist exclusively of pure rotational transitions with selection rule $\Delta K = 0$, the purely axial parameters ($A - B$), D_K , H_K appearing in Eq. (1) cannot be determined for the ground vibrational states, although they contribute to the transition frequencies measured for the $\nu_8 = 1, 2$ excited states, because the l -type resonance off-diagonal matrix element of Eq. (3) connects levels with

Table 1: Spectroscopic parameters^[a] of CD₃CP in the ground and $\nu_8 = 1, 2$ states.

Parameter	Unit	Ground state		$\nu_8 = 1$		$\nu_8 = 2^0$		$\nu_8 = 2^2$	
		Present	Ref. 3	Present	Ref. 3	Present	Ref. 3	Present	Ref. 3
$4g_u$	MHz							364110(298)	720000
$(A - B)$	MHz	75336.736 ^[b]	73300	75313.780 ^[b]	73300	75301.238 ^[b]	73300	75301.238 ^[b]	73300
B	MHz	4293.655419(49)	4293.6596(4)	4303.86605(26)	4303.846(5)	4313.35395(57)	4313.330(10)	4313.97271(57)	4313.954(10)
D_J	kHz	0.728907(12)	0.8	0.74471(84)		0.7604(19) ^[d]		0.7604(19) ^[d]	
D_{JK}	kHz	42.7445(22)	43.00(9)	43.0795(35)	43.79(56)	43.258(11)	44.43(63)	43.4072(89)	44.43(63)
D_K	MHz	0.7065 ^[c]		0.7065 ^[c]		0.7065 ^[c]		0.7065 ^[c]	
H_{JK}	Hz	0.12243(63) ^[d]		0.12243(63) ^[d]		0.12243(63) ^[d]		0.12243(63) ^[d]	
H_{KJ}	Hz	0.6234(69) ^[d]		0.6234(69) ^[d]		0.6234(69) ^[d]		0.6234(69) ^[d]	
$-2A_C$	MHz			-126864(111) ^[d]	-134548(5000)			-126864(111) ^[d]	-134548(5000)
η_J	kHz			75.861(35)	73.7(11)			76.762(28)	74.9(12)
η_{JK}	kHz			-0.00508(70)				-0.00513(70)	
q	MHz			5.05821(39)	5.058(6)			5.005(13)	5.058
No. of lines		176		109				97	
rms	kHz	16		11				18	
σ		0.98		0.75				0.73	

Notes: [a] Numbers in parentheses are one standard deviation in units of the least significant figures. Parameters without quoted uncertainties were kept fixed in the fits. Empty entries indicate parameter not applicable or not used in the fit. [b] Rotational constant A calculated using the semi-experimental equilibrium structure and theoretical vibro-rotational corrections. [c] Fixed to the *ab initio* computed value. [d] Parameters fitted keeping their value in different vibrational states fixed to a 1:1 ratio, according to the SPFIT procedure.

K values differing by ± 2 . For this reason A and D_K were constrained to values obtained using *ab initio* computed quadratic and cubic force constants (details are reported in the next section). The spectroscopic constants for the ground and the $\nu_8 = 1, 2$ states of CH₃CP were obtained through a global analysis of all microwave and IR data available, which are previously published cm-wave [3](#) and mm-wave [10](#) transition frequencies, new mm-wave data acquired in this work, and ro-vibrational transitions of the ν_8 fundamental and $2\nu_8 \leftarrow \nu_8$ hot-band recorded in the FIR region [11](#). These last data were given a weight corresponding to an uncertainty of 0.0002 cm^{-1} . The spectroscopic constants of the non-degenerate $\nu_4 = 1$ state of CH₃CP were obtained by the analysis of the mm-wave transitions measured in the 79–111 GHz and 258–289 GHz frequency ranges. The spectroscopic constants determined for the ground state, and for the $\nu_8 = 1, 2$, and $\nu_4 = 1$ excited states of CH₃CP are collected in Table [2](#). As expected, the values of the fitted parameters for the vibrational ground state are essentially identical to those obtained previously by pure rotational transitions [10](#), but significant changes are produced for some excited-state constants determined by FTIR spectroscopy [11](#) for the $\nu_8 = 1, 2$ states. Table [3](#) shows the comparison between new and previous sets of spectroscopic parameters of CH₃CP for the ground and $\nu_8 = 1, 2$ states. A graphical display of the trend of some spectroscopic constants (G_i) with the vibrational excitation is given in Fig. [4](#). For graphical reasons, the value of $\frac{|G_i - G_0|}{G_0}$ has been plotted instead of G_i . Only the parameters $B, D_{JK}, (A - B), D_J$ fitted in the ground, $\nu_8 = 1, \nu_8 = 2^0$, and $\nu_8 = 2^2$ states have been reported. A straight line passing through the ground state (origin of the axes) and $\nu_8 = 1$ points has been extrapolated to $\nu_8 = 2$ in order to check the trend across the vibrational excitation. The graph shows a consistent variation from $\nu_8 = 1$ to $\nu_8 = 2$. Extrapolated and experimental values of the constants do not match perfectly for $\nu_8 = 2$ because of the non-linear dependence on the vibrational quantum number and the $X_{ll}l^2$ term (see end of Section [3](#)). Additionally, these inconsistencies may be enhanced by the fact that some spectroscopic parameters had to be fixed at their *ab initio* values, thus affecting the value determined for other constants.

Two main reasons justify the differences between the two sets of constants: (i) we changed the assignments made by Bane *et al.* [11](#) for the rovibrational transitions of the $2\nu_8^0 \leftarrow \nu_8^{\pm 1}$ hot band, and (ii) we made different choices for the set of spectroscopic parameters in the least-squares analysis. Concerning the first issue, we re-assigned 41 wavenumbers of Ref. [11](#). They correspond to the $K = 0 \leftarrow 1$ transitions ($30 \leq J \leq 66$) of the R-branch, re-assigned as $K = 3 \leftarrow 2$ ($22 \leq J \leq 58$), and the $K = 3 \leftarrow 2$ transitions ($7 \leq J \leq 15$) of the Q-branch, re-assigned as different rovibrational transitions of the ν_8 fundamental band and the $2\nu_8 \leftarrow \nu_8$ hot-band manifold. Such choice was made after a careful analysis and was based on the overall quality of the global fit and the consistency of the obtained spectroscopic constants. Our choice of parameters to be fitted was slightly different from that of Ref. [11](#). The quartic centrifugal distortion constant D_K , fixed to zero in Ref. [11](#), was fixed to the theoretical value 2.92326 MHz for the ground state and fitted for the $\nu_8 = 1, 2$ states. The rotational constant A_0 was also fixed to the *ab initio* value 156837.4 MHz. As expected,

Table 2: Spectroscopic parameters^[a] of CH₃CP in the ground, $\nu_8 = 1, 2$ and $\nu_4 = 1$ states.

Parameter	Unit	Ground state	$\nu_8 = 1$	$\nu_8 = 2^0$	$\nu_8 = 2^2$	$\nu_4 = 1$
E_{vib}	cm ⁻¹		308.4025553(87)	602.45562(53)	625.584920(18)	
$(A - B)$	MHz	153646.06 ^[b]	153569.463(33)	153535.2(18)	153462.68(16)	
B	MHz	4991.342945(57)	5003.65657(12)	5014.87834(26)	5015.83512(21)	4978.59218(31)
D_J	kHz	0.996784(18)	1.018714(65)	1.05098(16)	1.04051(13)	0.99115(24)
D_{JK}	kHz	66.2370(16)	66.8390(90)	67.099(14)	67.386(13)	65.031(15)
D_K	MHz	2.92326 ^[c]	2.9285(11)	2.895(16) ^[d]	2.895(16) ^[d]	
H_{JK}	Hz	0.19782(29)	0.2051(41)	0.2119(60) ^[d]	0.2119(60) ^[d]	0.19782 ^[e]
H_{KJ}	Hz	1.7616(76)	2.68(11)	3.63(18) ^[d]	3.63(18) ^[d]	1.7616 ^[e]
$-2A\zeta$	MHz		-279431.07(14)		-279412.64(22)	
η_J	kHz		111.844(31)		113.408(29)	
η_K	MHz		10.8816(76)		10.979(50)	
τ_J	Hz		-0.389(15) ^[d]		-0.389(15) ^[d]	
τ_{JK}	kHz		-0.01814(57)		-0.02760(62)	
q	MHz		6.32224(36)		6.22301(76)	
q_J	Hz		-11.08(18) ^[d]		-11.08(18) ^[d]	
No. of lines			2648			38
MW <i>rms</i>	kHz		22.1			28.5
IR <i>rms</i>	cm ⁻¹		1.3×10^{-4}			
σ			0.71			1.32

Notes: [a] Numbers in parentheses are one standard deviation in units of the least significant figures. Parameters without quoted uncertainties were kept fixed in the fits. Empty entries indicate parameter not applicable or not used in the fit. [b] Rotational constant A calculated using the semi-experimental equilibrium structure and theoretical vibro-rotational corrections. [c] Fixed to the *ab initio* computed value. [d] Parameters fitted keeping their value in different vibrational states fixed to a 1:1 ratio, according to the SPFIT procedure. [e] Fixed to the ground state value.

 Table 3: Spectroscopic parameters^[a] of CH₃CP in the $\nu_8 = 1, 2$ states compared to previous values.

Parameter	Unit	$\nu_8 = 1$		$\nu_8 = 2^0$		$\nu_8 = 2^2$	
		Present	Ref. [11]	Present	Ref. [11]	Present	Ref. [11]
E_{vib}	cm ⁻¹	308.4025553(87)	308.283739(11)	602.45562(53)	602.473756(60)	625.584920(18)	625.110928(17)
$(A - B)$	MHz	153569.463(33)	150021.4975	153535.2(18)	150065.284	153462.68(16)	149963.230
B	MHz	5003.65657(12)	5003.65518(41)	5014.87834(26)	5014.87545(20)	5015.83512(21)	5015.83664(82)
D_J	kHz	1.018714(65)	1.01807(13)	1.05098(16)	0.93060(33)	1.04051(13)	1.05656(37)
D_{JK}	kHz	66.8390(90)	66.730(32)	67.099(14)	67.85(11)	67.386(13)	62.71(15)
D_K	MHz	2.9285(11)		2.895(16) ^[b]		2.895(16) ^[b]	
H_{JK}	Hz	0.2051(41)	0.1440(99)	0.2119(60) ^[b]	0.19781	0.2119(60) ^[b]	0.19781
H_{KJ}	Hz	2.68(11)	1.7613	3.63(18) ^[b]	1.7613	3.63(18) ^[b]	1.7613
$-2A\zeta$	MHz	-279431.07(14)	-272310.93(12)			-279412.64(22)	-272332.66(14)
η_J	kHz	111.844(31)	110.550(62)			113.408(29)	122.22(12)
η_K	MHz	10.8816(76)	-0.8548(38)			10.979(50)	
τ_J	Hz	-0.389(15) ^[b]				-0.389(15) ^[b]	
τ_{JK}	kHz	-0.01814(57)				-0.02760(62)	-0.992(14)
q	MHz	6.32224(36)	6.3167(11)			6.22301(76)	-6.4024(75)
q_J	Hz	-11.08(18) ^[b]	-8.84(34)			-11.08(18) ^[b]	
q_K	Hz						97.3(16)
q_{KK}	Hz						-6.720(79)

Notes: [a] Numbers in parentheses are one standard deviation in units of the least significant figures. Parameters without quoted uncertainties were kept fixed in the fits. Empty entries indicate parameter not applicable or not used in the fit. [b] Parameters fitted keeping their value in different vibrational states fixed to a 1:1 ratio, according to the SPFIT procedure.

such changes produced significantly different values for η_K , $A\zeta$ and the vibrational energies. Moreover, we considered the choice of fitting q_K and q_{KK} in Ref. [11] inconsistent with the low values of K spanned in their dataset (only from 0 to 5). Therefore, we preferred to fix them to 0 and to fit q_J and τ_J for $\nu_8 = 2$, as done for $\nu_8 = 1$. For these excited vibrational states, it was possible to fit the sextic centrifugal distortion constants H_{JK} and H_{KJ} , because of the inclusion of mm-wave transitions in the data set. The output files

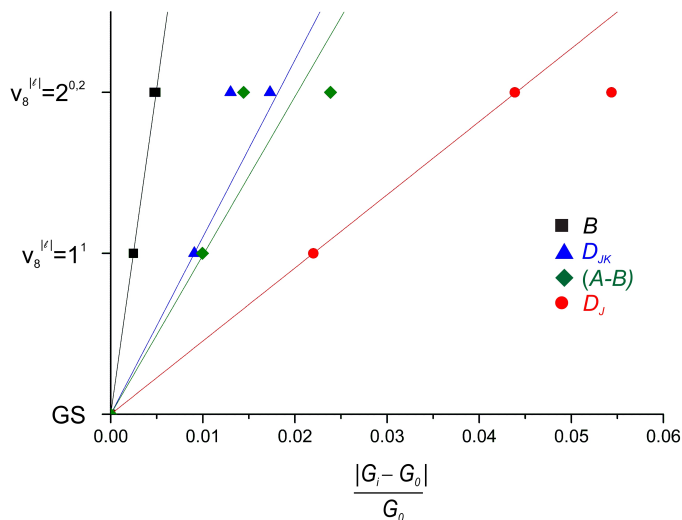


Figure 4: Variation of some normalized spectroscopic constants $[B, D_{JK}, (A-B), D_J]$ for the $v_8 = 1$ and $v_8 = 2$ states with respect to their corresponding ground state value. For graphical reasons, values for $(A-B)$ have been multiplied by a factor 20. See text for comments.

of SPFIT are deposited as supplementary material.

5. Semi-experimental equilibrium structure

Kroto *et al.* [3] were able to observe ground-state rotational transitions for eight isotopic species of 1-phosphapropyne in the 26–40 GHz frequency range, including also the asymmetrically substituted species CH_2DCP and CD_2HCP , for which both B_0 and C_0 rotational constants could be determined. Using all the information from the isotopic species observed, the substitution structure of 1-phosphapropyne was determined using both CH_3CP and CD_3CP as parent species. Fully experimental equilibrium structures are generally accessible for small molecules only [20]. Thus, in order to obtain the equilibrium structure of 1-phosphapropyne, we combined experimental results with *ab initio* calculations. First, we computed the potential energy surface near the minimum, so that reliable values of cubic and quartic force constants were obtained. This made it possible to remove computed zero-point vibrational contributions from experimental ground-state rotational constants, thus obtaining ten semi-experimental equilibrium rotational constants and consequently a semi-experimental equilibrium structure [21]. All quantum-chemical calculations reported in the present paper have been carried out using CFOUR [22]. The equilibrium structure has been obtained performing a geometry optimization at the coupled-cluster (CC) level of theory with single and double excitations [23], and a quasiperturbative treatment for triple substitutions [CCSD(T)] [24]. The correlation consistent polarized valence basis sets cc-pVTZ and cc-pVQZ [25] have firstly been employed in the frozen core (fc) approximation, then all electrons calculations (all) have also been considered with a basis set of triple- ζ quality. A further estimate of the equilibrium geometry have been obtained by making use of the additivity assumption for the core-valence (CV) correlation effects [26]. More precisely, the latter have been evaluated at the CCSD(T)/cc-pCVTZ level and added to the CCSD(T)/cc-pVQZ optimized geometry in the following way:

$$r_e(\text{CV-adj.}) = r(\text{fc-CCSD(T)/cc-pVQZ}) + \Delta r(\text{core/cc-pCVTZ}) \quad (4)$$

The theoretical estimates of the structural parameters of CH_3CP are reported in Table 4.

Table 4: Ab initio equilibrium structure of CH₃CP (bond lengths in Å and angle in degree).

	A(CCH)	R(C–H)	R(C–C)	R(C≡P)
CCSD(T)/cc-pVTZ (fc)	110.559	1.09190	1.47032	1.55923
CCSD(T)/cc-pCVTZ (all)	110.605	1.08843	1.46236	1.55432
CCSD(T)/cc-pVQZ (fc)	110.556	1.09091	1.46725	1.55295
Core-valence adjusted	110.602	1.08743	1.45929	1.54804

The harmonic and anharmonic (only cubic) force fields of 1-phosphapropyne have been evaluated employing the second-order Moller–Plesset perturbation theory (MP2) [27] in conjunction with the cc-pVTZ basis set. Vibration–rotation interaction constants α_r^i (where r denotes the vibrational mode ν_r and i the inertial axis) were then computed for each isotopic species by means of second-order perturbation theory [28]. Only eight experimental values of α_r^B constants are known for CH₃CP and CD₃CP isotopologues. They are listed in Table 5, where the corresponding MP2/cc-pVTZ theoretical values are also reported for comparison.

Table 5: Comparison between theoretical (MP2/cc-pVTZ) and experimental vibration-rotation interaction constants α_r^B (MHz) of the vibrational modes ν_r .

Isotopologue	Vibration	Theoretical	Experimental	Reference
CH ₃ CP	ν_2	34.6893	33.4622	[7]
CH ₃ CP	ν_3	14.5206	-15.256	[8]
CH ₃ CP	ν_4	13.0703	12.7493	This work
CH ₃ CP	ν_6	-7.9143	-3.256	[8]
CH ₃ CP	ν_7	3.1447	3.0980	[11]
CH ₃ CP	ν_8	-12.1441	-12.0745	This work
CD ₃ CP	ν_2	28.8503	27.404	[5]
CD ₃ CP	ν_8	-10.0463	-10.0559	This work

The agreement between experimental and theoretical values is generally satisfactory. Large discrepancies do only appear for α_3^B and for α_6^B constants of CH₃CP. This can be explained by considering that the ν_6 band was analyzed by Ohno *et al.* [8] taking into account a strong Coriolis interaction with ν_3 together with Coriolis and Fermi interactions with $\nu_4 + 2\nu_8$. For this reason the experimental, deperturbed α_3^B and α_6^B constants are not directly comparable with the theoretical ones, which were calculated using standard second-order perturbation theory. In addition, it must be pointed out that the results presented in Ref. [8] were entirely based on the analysis of vibration-rotation lines of the ν_6 band only, and no experimental datum directly related to the $\nu_3 = 1$ state was employed. A good agreement does also exist between theoretical and experimental ζ_{88} Coriolis coupling constants. Theoretical values are 0.8823 and 0.7992 for CH₃CP and CD₃CP, respectively, which compare well to those derived from the $A\zeta$ constant fitted for the $\nu_8 = 1$ states, which is 0.8811 for CH₃CP and 0.7967 for CD₃CP. Theoretical vibration–rotation coupling constants α_i^B have been used to calculate the equilibrium values B_e from the ground state B_0 rotational constants:

$$B_e = B_0 + \frac{1}{2} \sum_i \alpha_i d_i = B_0 + \Delta B_0 \quad (5)$$

where d_r is a degeneracy factor (1 for stretching and 2 for bending modes). An analogous expression has been used to calculate C_e for the asymmetrically substituted species CH₂DCP and CD₂HCP. In principle, a more accurate determination of the equilibrium constants should include the electronic contribution to the rotational constants, not reported in Eq. (5). Such electronic correction can be directly evaluated from the rotational \mathbf{g} tensor and the ratio between electron and proton masses [29]. We computed the rotational

\mathbf{g} tensor of each isotopologue at the MP2/aug-cc-pVTZ level of theory and subtracted the electronic contribution from the ground state constants. This newly determined semi-experimental equilibrium structure is equivalent to that derived without considering the electronic correction. This is consistent with the fact that: (i) the electronic contributions to the rotational constants B and C are very small, i.e., around 30–40 kHz for each isotopologues and (ii) the error in the computed vibrational corrections can be estimated of the order of some hundreds of kHz, much higher than the electronic corrections. For these reasons we did not include the electronic contributions in the derivation of the equilibrium rotational constants. Experimental B_0 and C_0 constants, theoretical ΔB_0 and ΔC_0 , and semi-experimental B_e and C_e constants are collected in Table 6 for the various isotopologues of 1-phosphapropyne.

Table 6: Ground-state rotational constants $G = B, C$, theoretical ro-vibrational corrections (MP2/cc-pVTZ), and semi-experimental equilibrium rotational constants (MHz).

Isotopologue	G	Ground-state	Reference	ΔG_0	G_e
CH ₃ CP	B	4991.34295	[10]	15.246	5006.5890
¹³ CH ₃ CP	B	4823.6545	[10]	14.303	4837.9575
CH ₃ ¹³ CP	B	4982.6194	[10]	15.070	4997.6894
CD ₃ CP	B	4293.65542	This work	13.939	4307.5944
¹³ CD ₃ CP	B	4182.9400	[3]	13.247	4196.1870
CD ₃ ¹³ CP	B	4290.2190	[3]	13.790	4304.0090
CH ₂ DCP	B	4749.172	[3]	14.125	4763.2970
CH ₂ DCP	C	4704.275	[3]	15.470	4719.7450
CD ₂ HCP	B	4519.339	[3]	13.757	4533.0960
CD ₂ HCP	C	4473.372	[3]	14.900	4488.2720

The equilibrium structure has been obtained by a least-squares fit of the structural parameters to the equilibrium moments of inertia I_e^i , derived from the corresponding semi-experimental equilibrium rotational constants. Four structural parameters (i.e., C–H, C–C, C≡P bond distances, and the \angle CCH angle) have been determined from a total of 10 moments of inertia. The quality of the fit is rather good with residuals for the moments of inertia never exceeding 1×10^{-4} amu \AA^2 , corresponding to observed – calculated values always lower than 4 kHz for the rotational constants. Although no isotopic substitution is feasible for the P atom, the precision of the C≡P bond length is comparable with those of C–C and C–H distances. In fact, our fit employs data from 8 isotopologues, all giving information about the equilibrium moment of inertia along the z -axis. In addition, semi-experimental r_e structures are generally less affected by occasional lacks of isotopic substitution compared to r_s structures. The effectiveness of the ro-vibrational corrections employed has been tested by performing also a least-squares fit in which experimental ground-state moments of inertia have been used to determine the r_0 structure of 1-phosphapropyne. A clear worsening of the quality of the fitting procedure occurs, since the residuals increase nearly by a factor of 40. In this case, observed – calculated values greater than 100 kHz are produced for some rotational constants. The r_e and r_0 structural parameters determined by the two least-squares fittings are reported in Table 7 where they are compared with the theoretical core-valence adjusted estimates and with the r_s structure previously determined by Kroto *et al.* [3].

Table 7: Comparison between different evaluations of the molecular structure of 1-phosphapropyne (bond lengths in \AA and angles in degrees).

Parameter	Core-valence adjusted	r_e	r_0	r_s (Ref. [3])
R(C–C)	1.45929	1.461951(44)	1.4595(18)	1.465(3)
R(C–H)	1.08743	1.090214(33)	1.1065(13)	1.107(1)
\angle (CCH)	110.602	110.5613(14)	110.258(55)	110.30(9)
R(C≡P)	1.54804	1.545609(34)	1.5513(14)	1.544(4)

A satisfactory agreement is generally observed between semi-experimental equilibrium parameters and

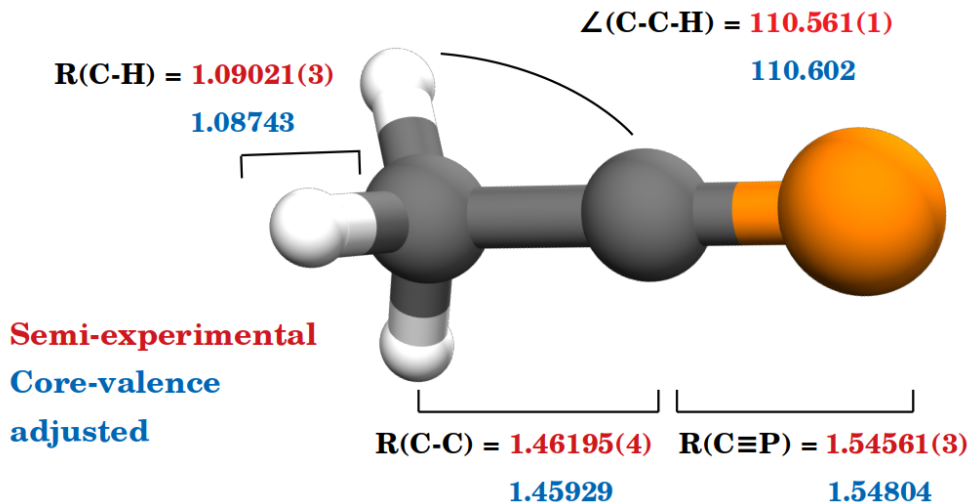


Figure 5: Semi-experimental and theoretical estimated equilibrium structure parameters of 1-phosphapropyne (bond lengths in Å and angles in degrees).

theoretical estimates, although the CCH angle and the CH bond length appear to be better reproduced by the CCSD(T)/cc-pVQZ calculation. Computation of the standard deviation for the calculated bond lengths with respect to the semi-experimental ones provides the lower value for the core-valence adjusted estimate (0.0030 Å) and higher values for the others (0.0034 Å for CCSD(T)/cc-pVQZ, 0.0055 Å for CCSD(T)/cc-pCVTZ, and 0.0060 Å for CCSD(T)/cc-pVTZ). As expected, neither r_0 , nor r_s structures are able to recover efficiently vibrational effects for distances and angles involving hydrogen atoms. A comparison between the semi-experimental and theoretical estimated equilibrium structures is displayed in Fig. 5

Table 8 summarizes a comparison between the semi-experimental equilibrium structure of 1-phosphapropyne and analogous structures of related species, containing either the $\text{C}\equiv\text{P}$ moiety (HCP, HC_3P , and NCCP) or a $\text{CH}_3\text{C-}$ group bound to a pnictogen element (CH_3CN).

Table 8: Comparison between semi-experimental r_e structural parameters of 1-phosphapropyne and those of related species (bond lengths in Å and angles in degrees).

Molecule	$R(\text{C}\equiv\text{P})$	$R(\text{C-C})$	$R(\text{C-H})$	$\angle(\text{CCH})$	Reference
CH_3CP	1.54561(3)	1.46195(4)	1.09021(3)	110.561(1)	This work
HCP	1.54008	30
HC_3P	1.5523(2)	31
NCCP	1.5456(3)	32
CH_3CN	...	1.4585(4)	1.0869(1)	109.84(1)	33

All the parameters reported in Table 8 were obtained from a semi-experimental equilibrium structure, so that some trends of the structural parameters can be highlighted. Firstly, the C-H bond length in CH_3CX increases passing from N to P, i.e., the smaller the electronegativity of X, the longer the C-H bond, as expected from elementary bond theory; the same is true for the (CCH) angle and for the C-C distance. Secondly, the $\text{C}\equiv\text{P}$ bond length appears to be poorly sensitive to the group (R-) which is bound to. Indeed, its value varies within a range of ~ 0.015 Å. The steric size of R and conjugation effects influence the $\text{C}\equiv\text{P}$ distance. This is confirmed by Natural Bond Orbital (NBO) analysis performed for all phosphorous-containing molecules of Table 8 at MP2/6-311G++(d,p) level of theory. While HCP shows negligible conjugation effects, the stabilization energy due to conjugation of the $\text{C}\equiv\text{P}$ group with methyl, cyano, and alkynyl substituents is smaller in CH_3CP than NCCP and HC_3P .

6. Conclusions

The rotational spectrum of CD₃CP in the ground, $\nu_8 = 1$ and $\nu_8 = 2$ vibrational states have been thoroughly re-investigated extending the measurements to the mm- and submm-wave regions. The precision of the centrifugal distortion constants of CD₃CP is now comparable with that of the parent species CH₃CP. As to the vibrational excited states of CD₃CP, the new mm-wave measurements allowed us to probe rotational levels with J values in the range 8–14, so that much larger splittings due to l -type doubling could be measured. Most of the related parameters were determined with considerable better precision, including also the vibrational energy difference between the $\nu_8 = 2^2$ and $\nu_8 = 2^0$ states. Several mm-wave lines have also been recorded up to 330 GHz for low-lying excited states of CH₃CP, and a global analysis including all available rotational [3, 10] and rovibrational transitions [11] related to the ground, $\nu_8 = 1$ and $\nu_8 = 2$ states has been performed. A satisfactory fit was obtained by changing the previous assignments for the 41 transition wavenumbers measured for the $2\nu_8^0 \leftarrow \nu_8^{\pm 1}$ hot band [11].

Finally, a semi-experimental equilibrium structure has been derived for CH₃CP and its structural parameters compared with related species. The newly determined equilibrium structure agrees well with the *ab initio* structure calculated at the CCSD(T) level of theory using a basis set of quadruple- ζ quality and the core-valence correlation energy gradient correction using the cc-pCVTZ basis set.

7. Acknowledgement

This study was supported by Bologna University (RFO funds) and by MIUR (Project PRIN 2015: STARS in the CAOS, Grant Number 2015F59J3R).

References

- [1] M. J. Hopkinson, H. Kroto, J. Nixon, N. Simmons, The detection of the reactive molecule 1-phosphapropyne, CH₃CP, by microwave spectroscopy, *Chem. Phys. Lett.* 42 (3) (1976) 460–461.
- [2] N. Westwood, H. Kroto, J. Nixon, N. Simmons, Formation of 1-phosphapropyne, phosphinetriylethane or ethyldynephosphine CH₃CP, by pyrolysis of dichloro (ethyl) phosphine-he (i) photoelectron spectroscopic study, *J. Chem. Soc. - Dalton Transactions* (9) (1979) 1405–1408.
- [3] H. Kroto, J. Nixon, N. Simmons, The microwave spectrum of 1-phosphapropyne, CH₃CP: molecular structure, dipole moment, and vibration-rotation analysis, *J. Mol. Spectrosc.* 77 (2) (1979) 270–285.
- [4] K. Ohno, H. Matsuura, H. Murata, An infrared study of 1-phosphapropyne, *J. Phys. Chem.* 88 (3) (1984) 342–344.
- [5] K. Ohno, Y. Yamamoto, H. Matsuura, H. Murata, Infrared study on the C≡P stretching vibration of 1-phosphapropyne CH₃CP and its perdeuterium analog CD₃CP, *Chem. Lett.* 13 (3) (1984) 413–414.
- [6] K. Ohno, H. Matsuura, D. McNaughton, H. W. Kroto, Infrared spectra of 1-phosphapropyne, CH₃CP, and its perdeuteride, CD₃CP, *J. Mol. Spectrosc.* 111 (2) (1985) 415–424.
- [7] K. Ohno, H. Matsuura, D. McNaughton, H. W. Kroto, The ν_2 infrared band of 1-phosphapropyne CH₃CP, *J. Mol. Spectrosc.* 124 (1) (1987) 82–91.
- [8] K. Ohno, H. Matsuura, D. McNaughton, H. W. Kroto, The ν_6 infrared band of 1-phosphapropyne CH₃CP, *J. Mol. Spectrosc.* 126 (2) (1987) 245–254.
- [9] K. Ohno, H. Matsuura, The ν_8 infrared band of ethyldynephosphine CH₃CP and its perdeuteride CD₃CP, *Bulletin of the Chemical Society of Japan* 60 (6) (1987) 2265–2267.
- [10] L. Bizzocchi, L. Cludi, C. Degli Esposti, Accurate quartic and sextic centrifugal distortion constants of CH₃CP, *J. Mol. Spectrosc.* 218 (1) (2003) 53–57.
- [11] M. K. Bane, C. Jones, S. L. Choong, C. D. Thompson, P. D. Godfrey, D. R. Appadoo, D. McNaughton, High-resolution FTIR spectroscopy of the ν_7 and ν_8 bands of 1-phosphapropyne, *J. Mol. Spectrosc.* 275 (2012) 9–14.
- [12] M. Melosso, A. Melli, C. Puzzarini, C. Codella, L. Spada, L. Dore, C. Degli Esposti, B. Lefloch, R. Bachiller, C. Ceccarelli, et al., Laboratory measurements and astronomical search for cyanomethanimine, *Astron. Astrophys.* 609 (2018) A121.
- [13] A. Melli, M. Melosso, N. Tasinato, G. Bosi, L. Spada, J. Bloino, M. Mendolicchio, L. Dore, V. Barone, C. Puzzarini, Rotational and infrared spectroscopy of ethanimine: a route toward its astrophysical and planetary detection, *Astrophys. J.* 855 (2) (2018) 123.
- [14] M. Melosso, B. A. McGuire, F. Tamassia, C. Degli Esposti, L. Dore, Astronomical search of vinyl alcohol assisted by submillimeter spectroscopy, *ACS Earth and Space Chemistry* 3 (7) (2019) 1189–1195.
- [15] M. Melosso, C. Degli Esposti, L. Dore, Terahertz spectroscopy and global analysis of the rotational spectrum of doubly deuterated amidogen radical ND₂, *Astrophys. J., Suppl. Ser.* 233 (1) (2017) 15.
- [16] R. Gordy, W & Cook, *Microwave molecular spectra*, Wiley, 1984.

- [17] M. Gnida, H. Mäder, H. Harder, A. Huckauf, L. Margulès, J. Cosléou, J. Demaison, P. Pracna, K. Sarka, The rotational spectrum of SiHF₃ in the vibrational state $v_6=2$: observation of direct l-type resonance transitions, *J. Mol. Spectrosc.* 216 (2) (2002) 481–492.
- [18] G. Wlodarczak, R. Bocquet, A. Bauer, J. Demaison, The submillimeter-wave rotational spectrum of propyne: analysis of the ground and the low-lying excited vibrational states, *J. Mol. Spectrosc.* 129 (2) (1988) 371–380.
- [19] H. Pickett, The fitting and prediction of vibration-rotation spectra with spin interactions, *J. Mol. Spectrosc.* 148 (2) (1991) 371–377.
- [20] M. Melosso, L. Bizzocchi, F. Tamassia, C. Degli Esposti, E. Canè, L. Dore, The rotational spectrum of ¹⁵ND. isotopic-independent dunham-type analysis of the imidogen radical, *Phys. Chem. Chem. Phys.* 21 (7) (2019) 3564–3573.
- [21] P. Pulay, W. Meyer, J. E. Boggs, Cubic force constants and equilibrium geometry of methane from hartree-fock and correlated wavefunctions, *J. Chem. Phys.* 68 (11) (1978) 5077–5085.
- [22] CFOUR, a quantum-chemical program package by J.F. Stanton, J. Gauß, M.E. Harding, M.E.P.G. Szalay with contributions from A.A. Auer, R.J. Bartlett, U. Benedikt, C. Berger, D.E. Bernholdt, Y.J. Bomble, L. Cheng, O. Christiansen, M. Heckert, O. Heun, C. Huber, T.-C. Jagau, D. Jonsson, J. Jusélius, K. Klein, W.J. Lauderdale, D.A. Matthews, T. Metzroth, L.A. Mück, D.P. O’Neill, D.R. Price, E. Prochnow, C. Puzzarini, K. Ruud, F. Schiffmann, W. Schwalbach, S. Stopkowitz, A. Tajti, J. Vázquez, F. Wang, J.D. Watts and the integral packages MOLECULE (J. Almlöf and P.R. Taylor), PROPS (P.R. Taylor), ABACUS (T. Helgaker, H.J. Aa. Jensen, P. Jørgensen, and J. Olsen), and ECP routines by A. V. Mitin and C. van Wüllen. For the current version, see <http://www.cfour.de>.
- [23] G. D. Purvis III, R. J. Bartlett, A full coupled-cluster singles and doubles model: the inclusion of disconnected triples, *J. Chem. Phys.* 76 (4) (1982) 1910–1918.
- [24] K. Raghavachari, G. W. Trucks, J. A. Pople, M. Head-Gordon, A fifth-order perturbation comparison of electron correlation theories, *Chem. Phys. Lett.* 157 (6) (1989) 479–483.
- [25] T. H. Dunning Jr, Gaussian basis sets for use in correlated molecular calculations. i. the atoms boron through neon and hydrogen, *J. Chem. Phys.* 90 (2) (1989) 1007–1023.
- [26] M. Heckert, M. Kállay, J. Gauss, Molecular equilibrium geometries based on coupled-cluster calculations including quadruple excitations, *Mol. Phys.* 103 (15-16) (2005) 2109–2115.
- [27] C. Møller, M. S. Plesset, Note on an approximation treatment for many-electron systems, *Phys. Rev.* 46 (7) (1934) 618.
- [28] I. M. Mills, Vibration-rotation structure in asymmetric- and symmetric-top molecules, *Molecular spectroscopy: modern research* 1 (1972) 115.
- [29] M. Piccardo, E. Penocchio, C. Puzzarini, M. Biczysko, V. Barone, Semi-experimental equilibrium structure determinations by employing B3LYP/SNSD anharmonic force fields: validation and application to semirigid organic molecules, *J. Phys. Chem. A* 119 (10) (2015) 2058–2082.
- [30] C. Puzzarini, R. Tarroni, P. Palmieri, J. Demaison, M. L. Senent, Rovibrational energy levels and equilibrium geometry of HCP, *J. Chem. Phys.* 105 (8) (1996) 3132–3141.
- [31] L. Bizzocchi, C. Degli Esposti, P. Botschwina, Millimeter-wave spectroscopy of HC₃P isotopomers and coupled-cluster calculations: the molecular structure of phosphabutadiyne, *Chem. Phys. Lett.* 319 (3-4) (2000) 411–417.
- [32] L. Bizzocchi, C. D. Esposti, P. Botschwina, Millimeter-wave spectroscopy and coupled cluster calculations for NCCP, *J. Chem. Phys.* 113 (4) (2000) 1465–1472.
- [33] C. Puzzarini, G. Cazzoli, Equilibrium structure of methylcyanide, *J. Mol. Spectrosc.* 240 (2) (2006) 260–264.